

Modelling of Polymer Crystallization in Temperature Fields

Martin Burger* Vincenzo Capasso[◊] Gerhard Eder[◊]

* Industrial Mathematics Institute, Johannes Kepler Universität Linz, Altenbergerstr. 69, 4040 Linz, Austria.

[◊] MIRIAM, Dipartimento di Matematica, Università di Milano, Via Saldini 50, 20133 Milano, Italy. On leave at Industrial Mathematics Institute, Johannes Kepler Universität Linz.

[◊] Institute of Chemistry, Johannes Kepler Universität Linz, Altenbergerstr. 69, 4040 Linz, Austria.

Abstract

This paper is devoted to the mathematical modelling of polymer crystallization processes in a bounded region under heat transfer conditions, i.e. in time-dependent temperature fields. A stochastic model in a general setup is developed based on the theory of marked point processes, and a hybrid model on a macroscopic scale is derived using expected values.

The stochastic modelling part is supplemented by a detailed discussion of the relevant parameters and their dependence upon temperature. In the special case of one-dimensional crystallization a system of partial differential equations describing the evolution of temperature and of the degree of crystallinity is derived.

1 Introduction

Crystallization processes generally can be viewed as a superposition of at least two processes, a nucleation process describing the time and location of spots in the material where crystals start to grow, and a growth process of the nucleated crystals. Sometimes also a third process due to the improvement of the crystalline structure of the crystals, called secondary crystallization, is of importance.

With most polymers when crystallizing from the quiescent melt, the growth mechanism of the crystallites can be viewed as a deterministic process leading to so-called spherulites whose radial growth rates are independent of their individual radii, but usually quite strongly dependent upon the (local) temperature. In the special case of spatially homogeneous growth, which is the case when temperature variations within the material can be

ignored, one gets ball shaped crystals centered in the point of nucleation. The radius of such a spherulite at time of observation t reads, if nucleation occurred at time $s \leq t$:

$$r(t, s) = \int_s^t G(\tau) d\tau \quad (1.1)$$

with $G(t)$ being the time-dependent radial growth rate. The corresponding volume is given by

$$v(t, s) = \frac{4\pi}{3} r(t, s)^3. \quad (1.2)$$

Nucleation processes are much more difficult to observe directly with experiments. Morphologies of fully crystallized samples after spatially homogeneous cooling show that the assumption of Poissonian distribution is often valid. Under this condition the following kinetic equation for the degree of conversion ξ has been derived by Kolmogorov [16]:

$$\xi(t) = 1 - e^{-\int_0^t \alpha(s) v(t, s) ds}, \quad (1.3)$$

with $\alpha(t)$ the time-dependent nucleation rate describing the appearance of nuclei per unit of volume and time in the melt starting from time $t = 0$.

If the additional assumption is made, that G is a function of the (changing) temperature, which usually is the case in polymer melts, i.e.

$$G(t) = \tilde{G}(T(t)), \quad (1.4)$$

the time dependence of G is uniquely connected to the time dependence of T . As it is well-known, the growth speed as a function of temperature is a bell-shaped curve showing a maximum somewhere between the equilibrium melting point and the glass-transition temperature, reaching zero at both ends (cf.[24]).

If temperature gradients are not negligible, one gets non-homogeneous nucleation and non-homogeneous growth. Possible relations between the nucleation rate field $\alpha(x, t)$ and the temperature field $T(x, t)$ will be discussed in Chapter 2. For the growth process the situation becomes more complicated, since the local growth rate as given by the following adaptation of equation (1.4)

$$G(x, t) = \tilde{G}(T(x, t)) \quad (1.5)$$

in general leads to non-spherical shapes of crystallites. In a first-order theory with respect to temperature gradients it has been shown that one gets spherical crystallites again, whose centers, however, do not coincide with the points of nucleation and whose radii grow faster when compared with crystallites whose neighbourhood follows the same temperature history as that of the point of nucleation (cf.[11, 12, 21]).

In practice, crystallization processes occur almost always under non-isothermal conditions. That means that in a mathematical description the equation of heat conduction (including a heat source term due to the release of latent heat of crystallization) must be solved simultaneously with equations describing the kinetics of crystallization. Moreover, due to the low thermal conductivity of polymers, the latent heat of crystallization and the usually quite high exterior cooling rates as occurring in polymer processing, also temperature gradients can be of decisive importance. Thus the assumption of spatial homogeneity of the crystallization kinetics as used in the derivation of model (1.3) often contradicts the situation which one faces in industrial applications.

2 Mathematical Modelling

2.1 Nucleation Models

Whereas with polymers the modelling of the local crystallite growth as given by equation (1.5) with some material function \tilde{G} is quite well established at least in those cases which are accessible to direct experimental investigation, the situation is not as straightforward with nucleation. Already Avrami [1, 2, 3] discussed a few special cases for isothermal crystallization after an ideal quench. If one assumes in such a situation that the nucleation rate is given by a negative exponential distribution with respect to the time coordinate with some (constant) mean activation time τ and number of potentially activable nuclei N_V , one has

$$\alpha(t) = \frac{N_V}{\tau} e^{-\frac{t}{\tau}} \quad (2.1)$$

and $G = G_c = \text{const.}$ for $t \geq 0$.

In this case one gets for the degree of crystallization and the number of observable crystallites per unit of volume

$$\xi(t) = 1 - e^{-8\pi N_V G_c^3 \tau^3 e_4(-t/\tau)} \quad (2.2)$$

and

$$N_c(t) = N_V \int_0^{t/\tau} e^{-u - 8\pi N_V G_c^3 \tau^3 e_4(-u)} du, \quad (2.3)$$

where $e_4(z) = \sum_{i=4}^{\infty} \frac{z^i}{i!}$ is an exponential rest series.

The following limiting cases of $\alpha = \alpha_c = \text{const}$ (corresponding to $\tau \gg t$) and $\alpha = N_V \delta_0(t)$, where δ_0 is the Dirac function concentrated at $t = 0$ (corresponding to $\tau \rightarrow 0$) are of particular importance. They lead in the first case to

$$\xi(t) = 1 - e^{-\frac{\pi}{3} \alpha G_c^3 t^4} \quad (2.4)$$

and

$$N_c(t) = \frac{1}{4} \left(\frac{3\alpha^3}{\pi G^3} \right)^{\frac{1}{4}} \gamma \left(\frac{1}{4}, \frac{\pi}{3} \alpha G^3 t^4 \right) \quad (2.5)$$

with the incomplete gamma function $\gamma(a, x) = \int_0^x e^{-t} t^{a-1} dt$. In the second limiting case one obtains

$$\xi(t) = 1 - e^{-\frac{4\pi}{3} N_V G^3 t^3} \quad (2.6)$$

and

$$N_c(t) = N_V. \quad (2.7)$$

The most obvious way for modelling the nucleation rate under non-isothermal conditions would be the assumption

$$\alpha(x, t) = \tilde{\alpha}(T(x, t)) \quad (2.8)$$

with some material function $\tilde{\alpha}$. This model reduces for isothermal crystallization after quenching to equations (2.4) and (2.5). However, experimentally one finds with many different polymers, that under these conditions usually the latter model as given by equation (2.6) and (2.7) is valid. In addition, the number of spherulites N_V is often found to be a strong function of the temperature, to which the sample had been quenched. The straightforward corresponding generalization for this case reads:

$$\alpha(x, t) = \frac{d}{dt} \tilde{N}(T(x, t)) = \frac{d\tilde{N}}{dT}(T(x, t)) \frac{\partial T}{\partial t}(x, t) \quad (2.9)$$

with some material function \tilde{N} , which gives in view of equation (2.9) exactly the number of crystallites after isothermal crystallization following a jump in temperature to T .

A more general representation of $\alpha(x, t)$ can be given in terms of an activation time spectrum (cf. [9]), in analogy to the well-known relaxation time spectrum of viscoelasticity theory. In fact, at least three mechanisms can be expected, viz. thermal, athermal and heterogenous nucleation, where in the latter case various types of active centers can be expected on a solid particle (edges, holes, crystal surfaces). In such a description one has:

$$\alpha(x, t) = \sum_i N_i a_i(x, t), \quad \text{with } a_i(x, t) = \frac{1}{\tilde{\tau}_i(T(x, t))} e^{-\int_{-\infty}^t \frac{ds}{\tilde{\tau}_i(T(x, s))}}. \quad (2.10)$$

However, such an equation is quite useless in practice, since it contains too many parameter which could never be determined experimentally.

One practicable way being consistent with experimental results is the assumption of a variety of activation temperatures T_i , one for every type of nucleation, and to simplify equation (2.10) by replacing the various terms $a_i(x, t)$ by Dirac functions concentrated around

the times when the sample temperature T reaches the respective activation temperatures during cooling. In other words, the activation times $\tilde{\tau}_i$, which are all infinite at the melting point, jump from infinite to zero one by one, when their activation temperature is reached, i.e.

$$\tilde{\tau}_i = \begin{cases} \infty & \text{if } T > T_i \\ 0 & \text{if } T \leq T_i \end{cases} \quad (2.11)$$

It may be noted that for athermal nucleation this model can be particularly realistic because of the fact that growth starts in this type of nucleation around frozen-in fluctuations as soon as their fixed size becomes critical during cooling. Equation (2.11) directly leads to the nucleation model as given by equation (2.9) with

$$\tilde{N}(T) = \sum_j N_j I_{(-\infty, T_j)}(T). \quad (2.12)$$

Without further argumentation, such an approximation has been proposed by Van Krevelen [23].

2.2 The Stochastic Model of the Crystallization Process

Crystallization of polymers can be modelled using birth-and-growth stochastic processes. At some temperature below the melting point crystals appear in the amorphous phase stochastically in time and space (*nucleation process*), and immediately start growing until parts of their surfaces hit some other neighboring crystallite (*impingement*), thus forming part of a contact interface.

We assume that the nucleation process is modelled as a stochastic spatially marked point process (MPP) on the underlying probability space (Ω, \mathcal{F}, P) ,

$$N = \sum_{j=1}^{\infty} \epsilon(T_j, X_j), \quad (2.13)$$

where T_j is the time of occurrence of the j -th nucleation and X_j denotes the space location of the j -th nucleus. T_j is a random variable valued in \mathbf{R}_+ and X_j is random variable valued in a Borel set $E \subset \mathbf{R}^d$, $d = 1, 2, 3$. We shall denote by \mathcal{B}_+ the σ -algebra of Borel sets in \mathbf{R}_+ , and by \mathcal{C} the σ -algebra of Borel sets in E .

For any $t \in \mathbf{R}_+$ and $x \in E$, $\epsilon(t, x)$ denotes the Dirac measure on $\mathcal{B}_+ \times \mathcal{C}$, such that for any $B \in \mathcal{B}_+$ and $C \in \mathcal{C}$,

$$\epsilon(t, x)(B, C) = \begin{cases} 1 & \text{if } t \in B \text{ and } x \in C \\ 0 & \text{otherwise.} \end{cases} \quad (2.14)$$

As a consequence, N is an integer-valued random measure on $\mathcal{B}_+ \times \mathcal{C}$. The random variable $N(A)$ counts the number of nucleation events in the region $A \in \mathcal{B}_+ \times \mathcal{C}$ of time-space, i.e.,

$$N(A) = \text{card} \{ j \mid (T_j, X_j) \in A \}. \quad (2.15)$$

Its randomness derives from the randomness of the nucleation events (T_j, X_j) . The (deterministic) measure defined by the expected values

$$\Lambda(A) := E[N(A)], \quad A \in \mathcal{B}_+ \times \mathcal{C}, \quad (2.16)$$

is known as the *intensity measure* of N .

The process $\{ N_t := N([0, t] \times E) \mid t \in \mathbf{R}_+ \}$ is the (underlying) counting process of N ; for any $t \in \mathbf{R}_+$ it counts the number of all nucleation events up to time t . Given the underlying probability space (Ω, \mathcal{F}, P) , we assume that for every $\omega \in \Omega$, the trajectory

$$t \in \mathbf{R}_+ \mapsto N(t, \omega) \in \mathbf{N}$$

is cadlag (right continuous with left limits), nondecreasing (piecewise constant) and simple (with jumps of size one).

By $\{ \mathcal{F}_t \mid t \in \mathbf{R}_+ \}$ we denote the natural filtration (history) of the process

$$\mathcal{F}_t := \sigma(N([0, t] \times C, 0 \leq s \leq t, C \in \mathcal{C})). \quad (2.17)$$

Under usual (general) assumptions on the process N , it can be shown [5] that a real-valued random measure ν on $\mathcal{B}_+ \times \mathcal{C}$ exists, such that

- For all $C \in \mathcal{C}$: $t \mapsto \nu([0, t] \times C)$ is \mathcal{F}_t -predictable.
- For all $A \in \mathcal{B}_+ \times \mathcal{C}$: $E[\nu(A)] = \Lambda(A) = E[N(A)]$.

The random measure ν is called the stochastic intensity of the MPP N . Under the usual assumptions on N , ν has the following representation:

$$\nu(dt \times dx) = E[N(dt \times dx) | \mathcal{F}_{t-}], \quad (2.18)$$

so that

$$\begin{aligned} \Lambda(dt \times dx) &= E[N(dt \times dx)] \\ &= E[E[N(dt \times dx) | \mathcal{F}_{t-}]] \\ &= E[\nu(dt \times dx)] \end{aligned} \quad (2.19)$$

The stochastic intensity of the underlying counting process $\{ N_t \mid t \in \mathbf{R}_+ \}$ will be given by

$$\tilde{\nu}(dt) := \nu(dt \times E) = \int_E \nu(dt \times dx). \quad (2.20)$$

It represents the nucleation rate in time referred to the whole available space E . A model for our crystallization process is specified by the stochastic intensity ν of the MPP N .

Let us denote by Θ^t the random closed set (RACS) that describes the region in E occupied by the crystalline phase, up to time $t \in \mathbf{R}_+$ (cf. [6]). As a consequence of the discussion in Section 2.1 we can assume that

$$\nu(dt \times dx) = \alpha(x, t)(1 - I_{\Theta^t-}(x))dxdt, \quad (2.21)$$

where $\alpha(x, t)$ is the mean number of new nuclei produced per unit volume and unit time at $(x, t) \in E \times \mathbf{R}_+$. This means that the nucleation itself is independent of the actual crystalline phase Θ^{t^-} .

If we denote by

$$\xi(x, t) := E[I_{\Theta^t}(x)] = P(x \in \Theta^t), \quad x \in E, t \in \mathbf{R}_+ \quad (2.22)$$

the crystallinity function, the intensity measure of the nucleation process N is given by

$$\begin{aligned} \Lambda(dt \times dx) &= E[N(dt \times dx)] \\ &= E[\alpha(x, t)(1 - I_{\Theta^{t^-}}(x))dxdt] \\ &= \alpha(x, t)(1 - \xi(x, t))dxdt. \end{aligned} \quad (2.23)$$

The average number of nuclei per unit volume born up to time $t \in \mathbf{R}_+$ at $x \in E$ will be given by

$$N_c(x, t) = \int_0^t \alpha(x, \tau)(1 - \xi(x, \tau))d\tau. \quad (2.24)$$

On the other hand, the stochastic intensity will be given by

$$\begin{aligned} \tilde{\nu}(dt) &= \int_E \alpha(x, t)(1 - I_{\Theta^{t^-}}(x))dxdt \\ &= \left(\int_{E - \Theta^t} \alpha(x, t)dx \right) dt. \end{aligned} \quad (2.25)$$

At any time $t \in \mathbf{R}_+$ the space-region $\Theta^t \subset E$ occupied by the crystalline phase is a random closed set (cf.[6]) on the probability space (Ω, \mathcal{A}, P) . A RACS Θ^t is completely characterized by its hitting function T_{Θ^t} defined on the compact sets of E by

$$T_{\Theta^t}(K) = P(\Theta^t \cap K \neq \emptyset), \quad K \subset E, K \text{ compact}. \quad (2.26)$$

In particular for $K = \{x\}$, $x \in E$, it gives the crystallinity function

$$\begin{aligned} T_{\Theta^t}(\{x\}) &= P(\Theta^t \cap \{x\} \neq \emptyset) \\ &= P(x \in \Theta^t) \\ &= E[I_{\Theta^t}(x)] \\ &= \xi(x, t). \end{aligned} \quad (2.27)$$

If we denote by $\Theta^t(T_j, X_j)$ the crystal born at (random) time $T_j \in \mathbf{R}_+$ and (random) location $X_j \in E$, freely grown up to time $t \geq T_j$, the overall crystallized region of E is given by

$$\Theta^t = \bigcup_{T_j \leq t} \Theta^t(T_j, X_j). \quad (2.28)$$

From the definition the degree of crystallinity at $(x, t) \in E \times \mathbf{R}_+$ is given by

$$\begin{aligned}\xi(x, t) &= P(x \in \Theta^t) \\ &= P(\exists j \in \mathbf{N} : x \in \Theta^t(T_j, X_j)).\end{aligned}\tag{2.29}$$

Viceversa, the probability that a point $x \in E$ is *not occupied* by the crystalline phase up to time $t \in \mathbf{R}_+$ is given by

$$\begin{aligned}p_x(t) &= 1 - \xi(x, t) \\ &= P(x \notin \Theta^t) \\ &= P(\forall j \in \mathbf{N} : x \notin \Theta^t(T_j, X_j)).\end{aligned}\tag{2.30}$$

A useful concept for evaluating the crystallinity $\xi(x, t)$ (and the survival probability $p_x(t)$) is given by the following definition:

Definition 2.1. The *causal cone* of a point $(x, t) \in E \times \mathbf{R}_+$ is the space-time region $A(x, t) \in \mathcal{B}_+ \times \mathcal{C}$ in which at least one nucleation has to take place such that point x is covered by the crystalline phase by time t :

$$A(x, t) := \{ (y, s) \in E \times \mathbf{R}_+ \mid x \in \Theta^t(y, s) \}.\tag{2.31}$$

If we assume that (cf.[7])

$$P(x \notin \Theta^t) = P(A(x, t) \cap N = \emptyset)\tag{2.32}$$

then

$$\begin{aligned}\xi(x, t) &= 1 - p_x(t) = 1 - P(x \notin \Theta^t) \\ &= 1 - e^{-\Lambda_0(A(x, t))},\end{aligned}\tag{2.33}$$

where

$$\begin{aligned}\Lambda_0(A(x, t)) &= E[N(A(x, t)) \mid \Theta^t \cap A(x, t) = \emptyset] \\ &= \int \int_{A(x, t)} \alpha(y, s)(1 - I_\emptyset(x)) dy ds \\ &= \int_0^t \left(\int_{\mathcal{E}(x, t, s)} \alpha(y, s) dy \right) ds\end{aligned}\tag{2.34}$$

with $\mathcal{E}(x, t, s)$ is defined by

$$\begin{aligned}\mathcal{E}(x, t, s) &= \{ y \in E \mid (y, s) \in A(x, t) \} \\ &= \{ y \in E \mid x \in \Theta^t(y, s) \}\end{aligned}\tag{2.35}$$

Remark 2.2. It can be shown (cf.[7]) that assumption (2.32) holds whenever the growth rate $G(x, t)$ is a function of location and absolute time $t \in \mathbf{R}_+$, as a consequence of an existence and uniqueness theorem applied to the growth lines of a crystal. In particular it holds whenever G is a function of the temperature $T(x, t)$ and no memory- or age-effects are present in the growth of crystals.

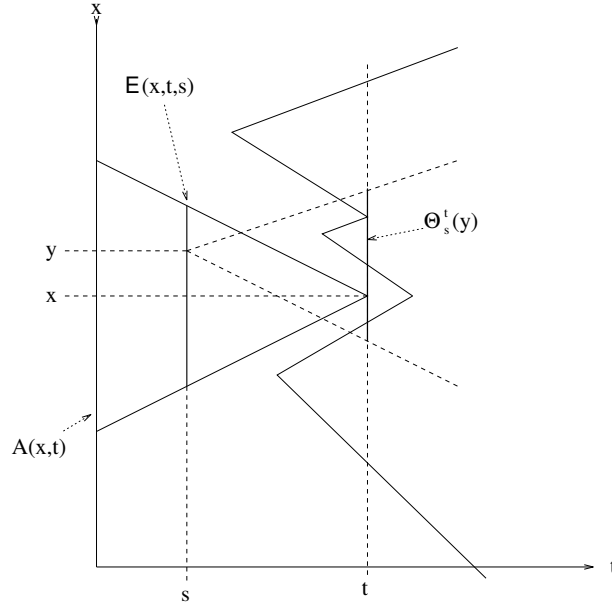


Figure 1: Causal cone in the case of constant growth rate in $E = \mathbf{R}^1$.

2.3 Growth Rates and Causal Cone

In the classical theory by Kolmogorov (1.3) the causal cone had a very special structure, in which the quantity in the exponent, i.e. $V_{ex}(t) = -\ln(1 - \xi(t))$ usually called the extended volume fraction, is also equal to the volume fraction at time $t \geq 0$ of all the crystals (born up to time t in the absence of impingement). In the case of space-heterogeneity this is obviously not true, because the causal cone of a point x is now determined by the growth of nuclei born at locations with possibly different evolution of the growth rate. Nevertheless the equations for the homogenous case are often used for nonisothermal applications without any changes. Almost all recent models for non-isothermal crystallization neglect the use of growth and nucleation properties at different locations which may influence the local quantity $\xi(x, t)$, so the evolution of ξ is described by ODEs or integro-differential equations in time.

Let us denote by

$$\begin{aligned} v(x, t) &:= \Lambda_0(A(x, t)) \\ &= \int_0^t \int_{\mathcal{E}(x, t, s)} \alpha(y, s) dy ds, \end{aligned} \quad (2.36)$$

so that the degree of crystallinity is given by

$$\xi(x, t) = 1 - e^{-v(x, t)}. \quad (2.37)$$

This is an extension of the so-called Kolmogorov-Avrami-Evans formula (cf.[1, 2, 3, 15, 16]).

If we now denote by $\chi(x, t, y, s) := I_{\mathcal{E}(x, t, s)}(y)$ the indicator function of the section $\mathcal{E}(x, t, s)$, we may rewrite (2.36) as

$$v(x, t) = \int_0^t \int_E \chi(x, t, y, s) \alpha(y, s) dy ds. \quad (2.38)$$

Since the jump in the indicator function χ is propagated with speed G at $(y, s) \in E \times \mathbf{R}_+$, the function χ satisfies the (backward) growth equation

$$\frac{\partial \chi}{\partial s}(x, t, y, s) = G(y, s) \|\nabla_y \chi\|(x, y, t, s), \quad x, y \in E, s, t \in \mathbf{R}_+ \quad (2.39)$$

because the growth lines are just the characteristics of the above equation. Equation (2.39) is supplemented by the conditions

$$\chi(x, t, x, s) = 1, \quad x \in E, s, t \in \mathbf{R}_+, s < t, \quad (2.40)$$

$$\chi(x, t, y, t) = 0, \quad x, y \in E, t \in \mathbf{R}_+, x \neq y. \quad (2.41)$$

2.4 Coupling with the Equation of Heat Conduction

As explained in Chapter 1, the equations as derived above have to be coupled with a model for the evolution of temperature. Due to the release of latent heat during the crystallization process changes in the crystallinity of the material causes also changes in temperature, i.e., the time-derivative of ξ occurs as a source term in the heat equation:

$$\frac{\partial T}{\partial t} = a\Delta T + \frac{h}{c} \frac{\partial \xi}{\partial t} \quad \text{in } E \times \mathbf{R}_+. \quad (2.42)$$

This equation is already a simplification, because all parameters in the heat equation as the heat capacity, heat diffusivity and the density depend on the temperature and crystallinity or even on the actual morphology. Here we consider this dependence to be a second-order effect. The boundary conditions on T are determined by the kind of cooling. They satisfy a Robin-type condition

$$\alpha T(x, t) + \frac{\partial T}{\partial n}(x, t) = g(x, t) \quad \text{on } \partial E \times \mathbf{R}_+, \quad (2.43)$$

and initial values given by

$$T(x, 0) = T^0(x) \quad \text{in } E \times \{0\}, \quad (2.44)$$

with $T^0(x) \geq T_m$, where T_m is the thermodynamic melting point temperature.

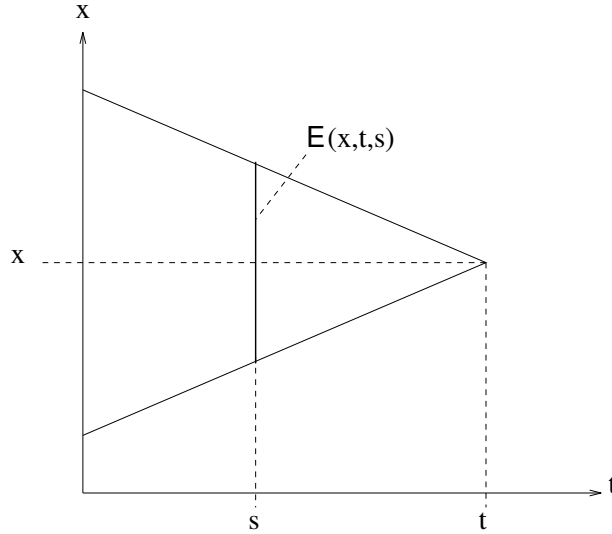


Figure 2: One-dimensional representation of the causal cone in the case of constant growth rate.

2.5 Crystallization in One Spatial Dimension

A more detailed analysis can be carried out in the one-dimensional case. We shall refer to this case from now on even though it is difficult to perform one-dimensional crystallization in practice (cf.[22]) and its practical importance is quite limited.

An ideal one-dimensional experiment could be imagined as crystallization in a fibre, in which the typical nearest neighbour distance of the nuclei is large as compared to the diameter of the fibre. Only in this case the spherulitic crystallization of the polymer appears to be like the crystallization of rodlike crystals. For the heat equation the one-dimensional version of equation (2.42) can be used, if the heat transfer from the fibre to its surroundings is negligibly small. This can, in principle, be achieved with an experiment, in which the polymer fibre is enclosed in a glass capillary with very thin walls, which itself is surrounded by vacuum. In this case heat flow, and thus also the temperature gradient, is in the fibre direction.

The growth equation (2.39) can now be rewritten as

$$\begin{aligned} \frac{\partial \chi}{\partial s}(x, t, y, s) &= G(y, s) \frac{\partial \chi}{\partial y}(x, t, y, s) & \text{if } y < x, \\ \frac{\partial \chi}{\partial s}(x, t, y, s) &= -G(y, s) \frac{\partial \chi}{\partial y}(x, t, y, s) & \text{if } y > x, \end{aligned} \quad (2.45)$$

This system of first-order PDEs for χ can be transformed into the second-order hyperbolic PDE

$$\begin{aligned} \frac{\partial \chi}{\partial s} &= G(y, s) \zeta \\ \frac{\partial \zeta}{\partial s} &= \frac{\partial}{\partial y} \left(G(y, s) \frac{\partial \chi}{\partial y} \right) & y \in E, s \in \mathbf{R}_+, \end{aligned} \quad (2.46)$$

with initial and boundary conditions

$$\begin{aligned}\chi(x, t, y, t) &= 0 & x, y \in E, t \in \mathbf{R}_+ \\ \frac{\partial \chi}{\partial s}(x, t, y, t) &= 2\delta(x - y) & x, y \in E, t \in \mathbf{R}_+\end{aligned}\quad (2.47)$$

where E is now a simple interval on the real line \mathbf{R} . The function $\frac{1}{2}\chi$ is just a Green's function of the hyperbolic problem. Using the symmetry of the problem one can deduce from (2.38) that v satisfies

$$\begin{aligned}\frac{\partial v}{\partial s} &= Gw \\ \frac{\partial w}{\partial t} &= \frac{\partial}{\partial x} \left(G(x, t) \frac{\partial v}{\partial x} \right) + 2\alpha(x, t) & \text{in } E \times \mathbf{R}_+\end{aligned}\quad (2.48)$$

with initial conditions

$$\begin{aligned}v(x, 0) &= 0 & \text{in } E \\ \frac{\partial v}{\partial x}(x, 0) &= 0 & \text{in } E.\end{aligned}\quad (2.49)$$

By direct computation we obtain the boundary condition

$$\begin{aligned}\frac{\partial v}{\partial t}(x, t) + G(x, t) \frac{\partial v}{\partial n}(x, t) &= \\ G(x, t) \left(w(x, t) + \frac{\partial v}{\partial n}(x, t) \right) &= 0, \text{ on } \partial E \times \mathbf{R}_+, \end{aligned}\quad (2.50)$$

which completes the modelling of the evolution equation for the causal cone. If $G(x, t) = 0$, the evolution equation degenerates to

$$\frac{\partial v}{\partial t} = 0. \quad (2.51)$$

In the following special case we are considering rates α and G given by material functions \tilde{N} and \tilde{G} by the following relations:

$$\alpha(x, t) = \max \left(-\frac{\partial}{\partial t} \left(\tilde{N}(T(x, t)) \right), 0 \right), \quad (2.52)$$

$$G(x, t) = \tilde{G}(T(x, t)). \quad (2.53)$$

The quantity v is related to the degree of crystallinity ξ via $v = -\ln(1 - \xi)$. Using these relations together with the one-dimensional heat-equation we end up with the following

initial-boundary value problem:

$$\begin{aligned}
\xi &= 1 - e^{-v} \\
\frac{\partial T}{\partial t} &= D \frac{\partial^2 T}{\partial x^2} + L e^{-v} \frac{\partial v}{\partial t} \\
\frac{\partial v}{\partial t} &= \tilde{G}(T)w && \text{in } E \times \mathbf{R}_+ \\
\frac{\partial w}{\partial t} &= \frac{\partial}{\partial x} \left(\tilde{G}(T) \frac{\partial v}{\partial x} \right) + 2 \max \left(\frac{\partial}{\partial t} \left(\tilde{N}(T) \right), 0 \right)
\end{aligned} \tag{2.54}$$

$$\begin{aligned}
T(x, 0) &= T^0(x) \\
v(x, 0) &= 0 \\
w(x, 0) &= 0
\end{aligned} \tag{2.55} \quad \text{in } E$$

$$\begin{aligned}
\alpha T(x, t) + \frac{\partial T}{\partial n}(x, t) &= \alpha T_1(x, t) \\
w(x, t) + \frac{\partial v}{\partial n}(x, t) &= 0
\end{aligned} \tag{2.56} \quad \text{on } \partial E \times \mathbf{R}_+$$

We note that \tilde{N} is a nonincreasing function. Hence, if the temperature is decreasing which is the case in practical applications, the maximum is of no importance, because $\tilde{N}(T(x, t))$ is increasing, i.e. the time derivative of w is nonnegative.

In short, from now on, system (2.54) - (2.56) will be called the *BCE-Model*.

2.6 Rate Equations

The model equation (2.54) turns out to be a generalization of the frequently used rate equations, which were first published by Schneider et al. [20] and derived from the classical Kolmogorov theory. Its one-dimensional equivalent with the special modelling of α is given by

$$\begin{aligned}
\frac{\partial v}{\partial t} &= \tilde{G}(T)w \\
\frac{\partial w}{\partial t} &= 2 \max \left(\frac{\partial}{\partial t} \left(\tilde{N}(T) \right), 0 \right)
\end{aligned} \tag{2.57} \quad \text{in } E \times \mathbf{R}_+$$

In the case where the spatial variations of \tilde{G} are small as compared to the variations of \tilde{N} in time (i.e. small temperature gradients), this equation is a good approximation of (2.54) - at least in the interior of the domain. The initial-boundary value problem for v resp. ξ may be interpreted as a singularly perturbed problem. General results about singularly perturbed problems let us expect a 'boundary layer', where the solutions of (2.54) and (2.57) differ significantly. This can also be seen from the numerical simulations in Section 4.

The differences at the boundary can easily be explained using the causal cone approach. In the classical Avrami-Kolmogorov approach the causal cone is the union of balls with radii $\int_s^t G(x, \tau) d\tau$. If the point x is close to the boundary, a big part of such a ball would lie outside E . It is possible, however, to derive a generalized Kolmogorov model, which includes this effect [10]. Also in the BCE-model this effect is included, since the causal cone is the union of the sets $\mathcal{E}(x, t, s)$ which are always subsets of E .

In higher dimensions it is not possible to derive a system of PDEs for ξ easily, but the behaviour of the solution is similar. The crucial point in numerical simulation is the approximation of the integrals $\int_{\mathcal{E}(x, t, s)} \alpha(y, s) dy$. If \tilde{G} is small the domains $\mathcal{E}(x, t, s)$ are also small, thus local linearizations can be used. The results in the one-dimensional case give the advice to incorporate the specific behaviour near the boundary into the simplified model.

The obvious approximation is the use of a localized version of the space-homogenous model equation, which reads:

$$v(x, t) = \omega_d \int_{-\infty}^t \alpha(x, s) \left(\int_s^t G(x, \tau) d\tau \right)^d ds, \quad (2.58)$$

where ω_d is the volume of the unit sphere in \mathbf{R}^d , $d = 1, 2, 3$. For the number of existing spherulites per unit volume one has:

$$N_c(x, t) = \int_{-\infty}^t \alpha(x, s) (1 - \xi(x, s)) ds. \quad (2.59)$$

This means that we approximate

$$\int_{\mathcal{E}(x, t, s)} \alpha(y, s) dy \approx \alpha(x, s) |\mathcal{E}(x, t, s)| \quad (2.60)$$

$$\approx \alpha(x, s) \omega_d \left(\int_s^t G(x, \tau) d\tau \right)^d, \quad (2.61)$$

which is reasonable, if the domains $\mathcal{E}(x, t, s)$ (or more precisely the growth rates) are small and if the temperature variation is small.

Using a method as originally used by Schneider et al. [20], instead of these equations an equivalent system of differential equations (the *rate equations*) can be employed, if the following auxiliary function is introduced:

$$\varphi_0(x, t) = -\ln(1 - \xi(x, t)). \quad (2.62)$$

The differential equations obtained read as follows:

$$\dot{\varphi}_{i-1}(x, t) = G(t) \varphi_i(x, t) \quad (2.63)$$

for $i = 1, \dots, d$, $\varphi_i(-\infty) = 0$ and

$$\dot{\varphi}_d(\mathbf{x}, t) = (d - 1)\omega_d\alpha(\mathbf{x}, t) \quad (2.64)$$

which has to be solved simultaneously with the model for the heat transfer given by (2.42)-(2.44). The heat source term in equation (2.42) is given by

$$\dot{\xi}(\mathbf{x}, t) = G(\mathbf{x}, t)\varphi_1(\mathbf{x}, t)e^{-\varphi_0(\mathbf{x}, t)} \quad (2.65)$$

which shows directly the coupling between the kinetic equations and the heat transfer.

For the development of the morphology one can use equation (2.59) in its differential form, which reads

$$\dot{N}_c(\mathbf{x}, t) = \alpha(\mathbf{x}, t)e^{-\varphi_0(\mathbf{x}, t)}. \quad (2.66)$$

Equation (2.65) gives a quite natural interpretation of the crystallization process, saying that the speed of crystallization is the product of the current growth speed and the free surface per unit of volume of the crystallites, which is $\varphi_1(1 - \xi)$.

In contrast to equation (2.65), the concepts of the isokinetic assumption ([18]) or time additivity (e.g.[8]) lead to the very popular form of kinetic equations as expressed by

$$\dot{\xi}(\mathbf{x}, t) = F(T(\mathbf{x}, t), \xi(\mathbf{x}, t)). \quad (2.67)$$

These models are not able to predict any structure development, since the speed of crystallization is determined in this class of models only by the current growth speed and the current degree of conversion, irrespective whether one has a rather fine grained or a very coarse grained structure.

Very often an even more crude model is used frequently in simulation, i.e. the so-called "enthalpy method" (cf. e.g. [17]). The base of this method is the assumption, that the degree of crystallinity is a pure temperature function, starting from zero at high temperatures to some constant limiting value at low temperatures:

$$\xi(t) = \tilde{\xi}(T(t)) \quad (2.68)$$

The heat equation (2.42) can be written in this case as:

$$\left(1 - \frac{h}{c_p} \frac{d\tilde{\xi}}{dT}(T(t))\right) \frac{\partial T}{\partial t} = a\Delta T \quad (2.69)$$

which is a diffusion equation with temperature dependent thermal coefficients, but without heat source term. However, everyone should be warned to use such a description, since any solidification kinetics is ignored in this case.

3 Parameter Identification

In practice one is interested in identifying kinetic parameters (material functions) from measurements of the temperature and observations of the morphology. With some polymers it is known from experiments that the assumptions of equations (1.4) and (2.9) are valid. In this case the identification of the parameters \tilde{G} and \tilde{N} , which fully characterize the crystallization behaviour of the material, is of great importance.

3.1 Experimental data

Many materials allow direct observation or indirect determination of the growth rate \tilde{G} (cf.[24, 19]). However, usually one has to cope with heat transfer problems even with standard experiments (cf.[13]), since small deviations in temperature have big influence on the kinetic parameters, in particular on the growth rate \tilde{G} . In Figure 3 the growth rate of isotactic polypropylene is reproduced from ref. [19]. The temperature sensitivity in the range of the higher temperatures is about one decade for a change of 12 degrees. Since in the equations for the degree of crystallinity (cf. subsection 2.1) always the third power of \tilde{G} shows up, this means, that an error in the temperature of 4 degrees changes the speed of crystallization by a factor 10 (!). Thus, in view of the low heat conductivity of polymers, one has to ensure a very accurate control of the temperature in experimentation. With other polymers (like e.g. polyethylene) the temperature sensitivity of \tilde{G} can even be higher than with polypropylene.

The growth rate data in Figure 3 is a compilation of data using quite different experimental methods like optical microscopy (high temperature range), optical observation of the movement of a crystallization zone in a steep temperature gradient and a light scattering technique (intermediate temperature range), and a quite tedious quench experiment using microtome cuts (full temperature range). Fortunately different grades of isotactic polypropylene (in a broad range of different molecular weights) show practically no difference in their growth rates with the exception of grades with very poor tacticity, which, however, are of no importance in practice.

For the nucleation data the situation is more complicated from the experimental point of view. One is often not able to obtain nucleation data directly from experiments, since it is usually not possible to quench samples quickly enough in order to get frozen-in morphologies from intermediate states. Due to the low heat conductivity of polymers this would only be possible for very thin samples, in which, however, one gets a change of the crystallization process due to the surfaces (cf. remarks after (2.57)) or due to additional surface nucleation, which takes place quite often in practice.

Figure 3 shows some nucleation data for an unnucleated isotactic polypropylene, which is a grade containing no nucleating agents, as one often has in processing to obtain higher crystallization speeds and more favourable final mechanical properties of the solidified product. Here again different experimental methods have been applied to get these data, which usually can not be determined very accurately. A main reason for this is that one always has to observe stochastic two-dimensional morphologies in a microtome cut from which nucleation data (for the threedimensional situation) are calculated. In the particular case which is shown in Figure 3 one has a change of one decade in the number of nuclei per 9 degrees change in temperature. This looks less dramatic than with the growth rate, since in the kinetic equations usually the first power of the nucleation rate shows up, in contrast to the third power of the growth rate. However, for an accurate determination of the final number of spherulites, which is an important quantity for the mechanical properties of a solidified sample, such a temperature sensitivity is quite high. Thus identification of the nucleation data is of special interest.

3.2 Identification of Nucleation and Growth Rates

Under suitable conditions, the model equation (2.37)-(2.44) in the time-interval $I = (0, t^*)$ and the special modelling of α and G as in (2.52), (2.53), admits a unique solution for given \tilde{N} and \tilde{G} , and thus the *parameter-to-output maps*

$$\begin{aligned} \mathcal{F} : \mathcal{D}(\mathcal{F}) &\rightarrow L^2(I) \times L^2(\Omega) \times L^2(\Omega) \\ \tilde{N} &\mapsto (T|_{\Gamma}, \xi|_{t=t_*}, \Lambda|_{t=t_*}) \end{aligned} \quad (3.1)$$

and

$$\begin{aligned} \mathcal{G} : \mathcal{D}(\mathcal{G}) &\rightarrow L^2(I) \times L^2(\Omega) \times L^2(\Omega) \\ \tilde{G} &\mapsto (T|_{\Gamma}, \xi|_{t=t_*}). \end{aligned} \quad (3.2)$$

may be defined.

The problem of estimating the nucleation rate may now be interpreted as the solution of the operator equation

$$\mathcal{F}(\tilde{N}) = (T_B^\delta, \xi_*^\delta) \quad (3.3)$$

and similary, the identification of the growth rate is equivalent to solving

$$\mathcal{G}(\tilde{G}) = (T_B^\delta, \xi_*^\delta) \quad (3.4)$$

The error of the measurement is denoted by δ . Due to the ill-posedness of the identification problem it is necessary to use a regularization method such as *Landweber-iteration* (cf.[14]). More details about the solution of the inverse problem for the one-dimensional case, i.e., parameter identification in the system (2.54) - (2.56) are given in [4].

4 Numerical Simulation of Crystallization processes

For the numerical simulation of a one-dimensional crystallization process with real data we suppose that crystallization occurs in a cylindric sample of 1 mm length and a diameter of 20 μm . This corresponds to isothermal experiments carried out by Schulze and Wilbert (cf.[22]) in a sample of similar size. The temperature range is chosen between 80° C and 130° C, where data about growth and nucleation rates for i-PP are accessible (cf.[19], see Figure 3). The diffusion coefficient is given by $a = 10^{-7} \text{ m}^2\text{s}^{-1}$, the temperature flux on the boundary is determined such that one achieves a cooling rate of around 10 Ks^{-1} , which is rather fast compared to typical DSC-experiments, but serves to demonstrate the special effects arising in the non-isothermal situation. The data for the latent heat is given by $L = \frac{h}{c} = 50 \text{ K}$.

A comparison of the results computed using the BCE-model (2.54)- (2.56) in Figure 4 and the ones of the Avrami-Kolmogorov model, which may be seen as the corresponding *reduced equation* in Figure 5 shows that the evolution of the temperature in the sample is

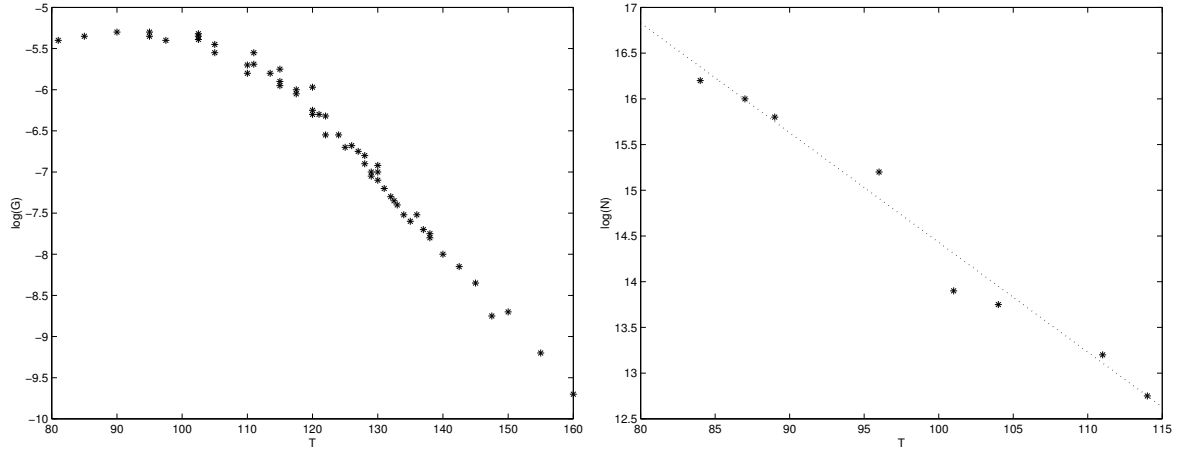


Figure 3: Measured values for \tilde{G} (in m/s) and \tilde{N} [m^{-3}] in logarithmic scale as functions of temperature T [$^{\circ}C$].

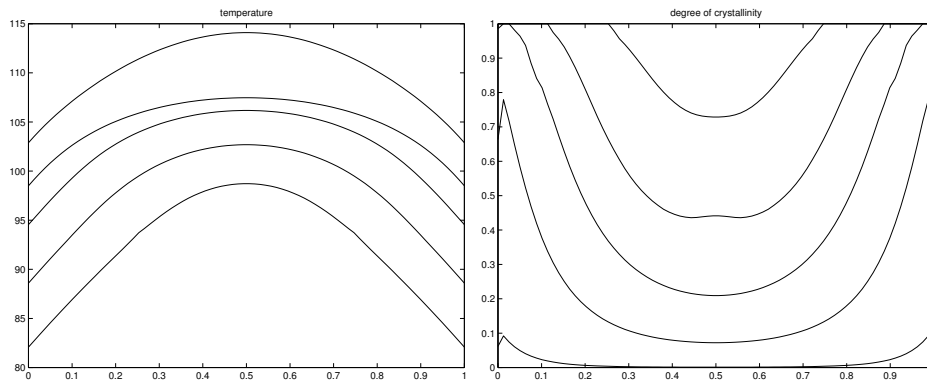


Figure 4: Temperature (in C) and degree of crystallinity after 2, 4, 6, 8 and 10 seconds as functions of the dimensionless fibre coordinate x as computed with model (2.54).

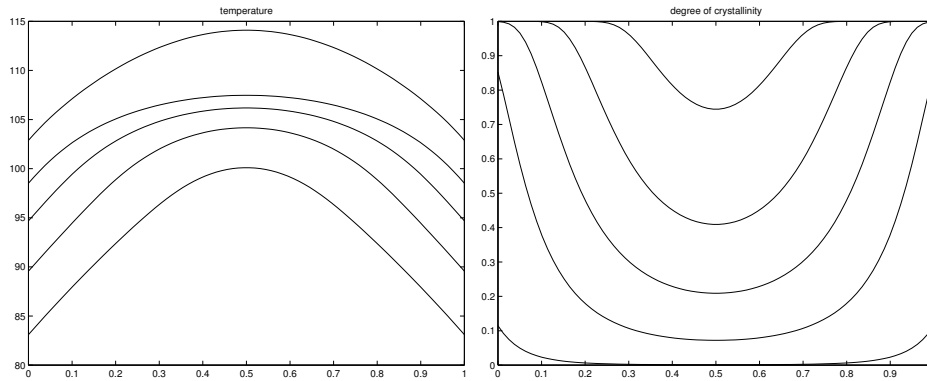


Figure 5: Temperature (in C) and degree of crystallinity after 2, 4, 6, 8 and 10 seconds as functions of the dimensionless fibre coordinate x as computed with the classical Avrami-Kolmogoroff model.

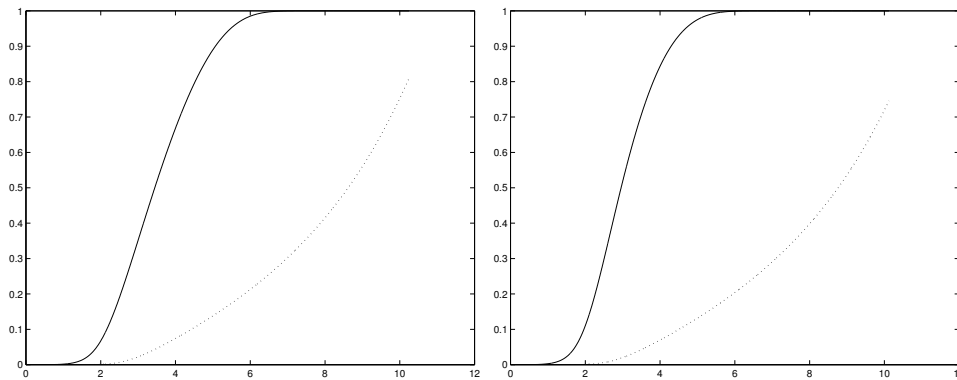


Figure 6: Evolution of the degree of crystallinity during the first 10 seconds near the boundary (solid) and in the middle of the sample (dotted), computed with model (2.54) (left) and the Avrami-Kolmogoroff model (right).

not affected significantly by the specific choice of the crystallization kinetic equation, while the influence of the latent heat can be seen clearly, especially between 6 and 8 seconds. As expected, the simplified Avrami-Kolmogorov model (2.58) leads to significant deviations in a boundary layer, which is due to the fact that it does not take into account the effect of *boundary impingement*.

The last Figure 6 shows the evolution of the degree of crystallinity for fixed location x close to the boundary of Ω and in the middle of the sample. Since the active cooling takes place at the boundary, the evolution of ξ in the middle of the sample is delayed. A comparison of both models shows again that there is no significant difference between the solutions in a certain distance from the boundary, while the simplified model predicts a faster increase of ξ near the boundary.

Acknowledgements

This work has been carried out in the framework of the ECMI Special Interest Group on Polymers, and has been partially supported by the EU under the TMR-Network *Differential Equations in Industry and Commerce* and by ASI, contract ARS-96-121. Useful and stimulating discussions are acknowledged with Hermann Janeschitz-Kriegl, Heinz W.Engl, Alessandra Micheletti and Claudia Salani.

References

- [1] M.Avrami, *Kinetics of phase change I*, J.Chem.Phys. **7**(1939), 1103-1112.
- [2] M.Avrami, *Kinetics of phase change II*, J.Chem.Phys. **8**(1940), 212-224.
- [3] M.Avrami, *Kinetics of phase change III*, J.Chem.Phys. **9**(1941), 177-184.
- [4] M.Burger, V.Capasso, H.W.Engl, *Inverse problems related to crystallization of polymers*, Technical Report 11/1998, Industrial Mathematics Institute, University of Linz (1998), to appear in *Inverse Problems*.
- [5] P. Brémaud, *Point Processes and Queues, Martingale Dynamics*. (Springer-Verlag, Heidelberg, 1981).
- [6] V.Capasso, M.DeGiosa, A.Micheletti, R.Mininni, *Stochastic modelling and statistics of polymer crystallization processes*, *Surveys on Mathematics for Industry* **6** (1996), 109-132.
- [7] V.Capasso, C.Salani, *Stochastic birth-and-growth processes modelling crystallization of polymers in a spatially heterogenous temperature field* (1998), in preparation.
- [8] T.V.Chan, G.D.Shyu and A.I.Isayev, *Master curve approach to polymer crystallization kinetics*, *Polym. Engng. Sci.* **35** (1995), 733 - 740.

- [9] G.Eder, H.Janeschitz-Kriegl, S.Liedauer *Crystallization processes in quiescent and moving polymer melts under heat transfer conditions*, Progr. Polym. Sci. **15**(1990), 629-714.
- [10] G.Eder, *Crystallization kinetic equations incorporating surface and bulk nucleation*, ZAMM Z.angew.Math.Mech. **76**(1996), S4, 489-492.
- [11] G.Eder, *Fundamentals of structure formation in crystallizing polymers*, in K.Hatada, T.Kitayama, O.Vogl, eds., *Macromolecular Design of polymeric Materials* (M.Dekker, New York, 1997), 761-782.
- [12] G.Eder, *Mathematical modelling of crystallization processes as occurring in polymer processing*, Nonlinear Analysis **30** (1997), 3807-3815.
- [13] G.Eder, *The Role of Heat Transfer Problems in Standard Crystallization Experiments*, in: Transport Phenomena in Polymer and Optical Fibre Processing, ASME HTD-Vol.**351** (1997), 131-137.
- [14] H.Engl, M.Hanke and A.Neubauer, *Regularization of Inverse Problems* (Kluwer, Dordrecht, 1996).
- [15] V.R.Evans, *The laws of expanding circles and spheres in relation to the lateral growth rate of surface films and the grain-size of metals*, Trans. Faraday Soc. **41** (1945), 365-374.
- [16] A.N.Kolmogorov, *On the statistical theory of the crystallization of metals*, Bull. Acad.Sci.USSR, Math.Ser. **1** (1937), 355-359.
- [17] W.Kurz, D.J.Fisher, *Fundamentals of Solidification*, Trans. Tech. Publ. Ltd., Aedermannsdorf, Switzerland, 1989.
- [18] K.Nakamura, T.Watanabe, K.Katayama and T.Amano, *Some aspects of nonisothermal crystallization of polymers I*, J. Appl. Polym. Sci. **16** (1972), 1077 - 1091.
- [19] E.Ratajski, H.Janeschitz-Kriegl, *How to determine high growth speeds in polymer crystallization*, Colloid Polym. Sci. **274** (1996), 938 - 951.
- [20] W.Schneider, A.Köppl, J.Berger, *Non-isothermal crystallization. Crystallization of polymers*, Intern. Polymer Processing **2** (1988), 151-154.
- [21] G.E.W.Schulze, T.R.Naujeck, *A growing 2D spherulite and calculus of variations*, Colloid & Polymer Science **269** (1991), 689-703.
- [22] G.E.W.Schulze, H.P.Wilbert, *Didactic experiment of a one-dimensional process of solidification at random to a linear polycrystal*, Colloid & Polym. Sci. **269** (1991), 981 - 992.

- [23] D.W. van Krevelen, *Crystallinity of polymers and the means to influence the crystallization process*, *Chimia* **32** (1978), 279-294.
- [24] D.W. van Krevelen, *Properties of Polymers*, (Elsevier Sci. Publ., Amsterdam, 1990).